

Communication

Crystallographic Orientation Relationship between α and β Phases during Non-Equilibrium Heat Treatment of Cu-37 wt. % Zn Alloy

Akbar Heidarzadeh ¹, Mousa Javidani ^{2,*} and Lyne St-Georges ^{2,*}

¹ Department of Materials Engineering, Azarbaijan Shahid Madani University, Tabriz 5375171379, Iran; ac.heydarzadeh@azaruniv.ac.ir

² Department of Applied Science, University of Québec at Chicoutimi, Saguenay, QC G7H 2B1, Canada

* Correspondence: Mousa_Javidani@uqac.ca (M.J.); Lyne_St-Georges@uqac.ca (L.S.-G.)

Abstract: The crystallographic orientation relationship between α and β phases during the non-equilibrium heat treatment of a Cu-37 wt. % Zn alloy was investigated. With this aim, Cu-37 wt. % Zn alloy plates with a thickness of 2 mm were heated at 810 °C for 1 h and then were quenched in water. The microstructure and texture of heat-treated samples were analyzed using optical microscopy and electron backscattered diffraction. By this non-equilibrium heat treatment, β phase was formed on both the grain boundaries and grain interiors. In addition, the $\Sigma 3$ twin boundaries acted as preferred areas for $\alpha \rightarrow \beta$ transformation. The orientation imaging microscopy results revealed a Kurdjumov–Sachs (K–S) orientation relationship between α and β phases. Furthermore, the details of microstructural evolution and texture analysis were discussed.

Keywords: crystallographic orientation relationship; heat treatment; microstructure; brass alloy



Citation: Heidarzadeh, A.; Javidani, M.; St-Georges, L. Crystallographic Orientation Relationship between α and β Phases during Non-Equilibrium Heat Treatment of Cu-37 wt. % Zn Alloy. *Crystals* **2022**, *12*, 97. <https://doi.org/10.3390/cryst12010097>

Academic Editors: Maria Cecilia Poletti, Silvana Sommadossi and Ricardo H. Buzolin

Received: 30 December 2021

Accepted: 11 January 2022

Published: 13 January 2022

Publisher's Note: MDPI stays neutral with regard to jurisdictional claims in published maps and institutional affiliations.



Copyright: © 2022 by the authors. Licensee MDPI, Basel, Switzerland. This article is an open access article distributed under the terms and conditions of the Creative Commons Attribution (CC BY) license (<https://creativecommons.org/licenses/by/4.0/>).

1. Introduction

Brasses are Cu–Zn alloys that contain different amounts of zinc, which have considerable applications in various industrial areas due to their special physical and mechanical properties. For example, they possess high thermal conductivity, considerable corrosion resistance, and a good combination of mechanical performances such as tensile strength and ductility [1]. It is notable that Zn plays the main role in determining the final properties of brasses, as it changes the microstructure at different concentrations. For example, at Zn < 37 wt. %, brasses only contain an α phase, which has a face-centered cubic (FCC) crystallographic structure. On the other hand, at Zn > 37 wt. %, the ordered β phase with a body-centered cubic (BCC) structure appears in brasses at room temperature, which causes an increase in strength. A disordered β phase transfers to an ordered β phase during equilibrium cooling at about 454 °C [2].

According to the Cu–Zn binary phase diagram [3] as shown in Figure 1, after equilibrium cooling of a Cu-37 wt. % Zn alloy, the microstructure only contains the α phase. This is due to the fact that an ordered β phase cannot be formed from an α phase. Therefore, one way to produce a double-phase structure in a Cu-37 wt. % Zn alloy is a non-equilibrium heat treatment in which the brass must be heated within the $\alpha + \beta$ zone, and the subsequent quenching should be applied to stabilize the disordered β phase at room temperature. Recently, Heidarzadeh et al. [2–4] used this technique to produce a double-phase structure in a Cu-37 wt. % Zn alloy before friction stir welding/processing (FSW/P). They showed that after FSW/FSP of α /disordered β brasses, novel composite structures such as nano and laminar composites can be produced.

Although in some studies, the α /disordered β brasses in Cu-37 wt. % Zn alloys have been friction stir welded/processed to produce novel structures, the fundamental information regarding the crystallographic orientation relationship between α and disordered

β phases is lacking, which can help us to control the microstructure and final mechanical properties of such alloys. With this in mind, in this study, orientation imaging microscopy (OIM) was utilized to disclose the orientation relationship between α and disordered β phases after non-equilibrium heat treatment.

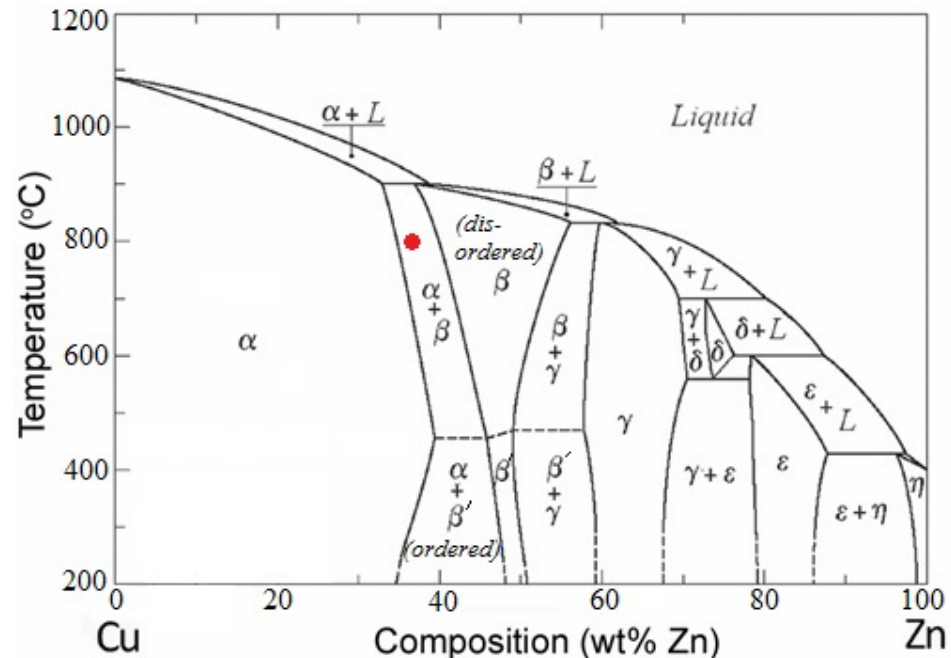


Figure 1. Cu–Zn binary phase diagram [3]. The area used for producing the α /disordered β double-phase brass is indicated by a red circle.

2. Materials and Methods

A single-phase brass plate containing 37 wt. % Zn with dimensions of 100 mm^{length} × 100 mm^{width} × 3 mm^{thickness} was used as the base material in this study. To produce the disordered β phase in α matrix, the base material was heat treated as follows. First, the single-phase plate was heated at 800 °C in an electrical furnace for 1 h. Then, the heated plate was quenched in water at room temperature (25 °C). The microstructures of the single-phase and double-phase samples were investigated using optical microscopy (OM). For this aim, the samples were cut from the single-phase and double-phase plates. Then, the mechanical polishing and etching with a solution of 50 mL of HCl, 10 mL of H₂O and 5 g of FeCl₃ was employed at room temperature (25 °C). A Philips XL30 E-SEM field emission gun scanning electron microscope (SEM) with an electron backscattered diffraction (EBSD) system was used to analyze the orientation relationships between α and disordered β phases. The EBSD samples were electro-polished in 250 mL of H₃PO₄, 250 mL of ethanol, 50 mL of propanol, 500 mL of distilled water and 3 g of urea at 10 V and 25 °C. The EBSD scans were obtained using a step size of 100 nm. EBSD data were analyzed using TSL OIM software. Moreover, the phase identification was confirmed using X-ray diffraction (XRD).

3. Results

The OM images of the single-phase (before heat treatment) and double-phase (after heat treatment) brasses at low and high magnifications are shown in Figure 2. According to Figure 2a,b, the single-phase plate had large grains of α (FCC) phase containing lots of annealing twins. After non-equilibrium heat treatment (described in the previous section), α grains were grown to some extent, and another phase was formed at the primary α grain boundaries and interiors (Figure 2c,d). In addition, the XRD patterns of single-phase and double-phase samples are illustrated in Figure 3. The observation of a β (110) peak after

heat treatment in the double-phase sample (Figure 3) confirms that β phase was formed from α phase during heat treatment (Figure 2c,d).

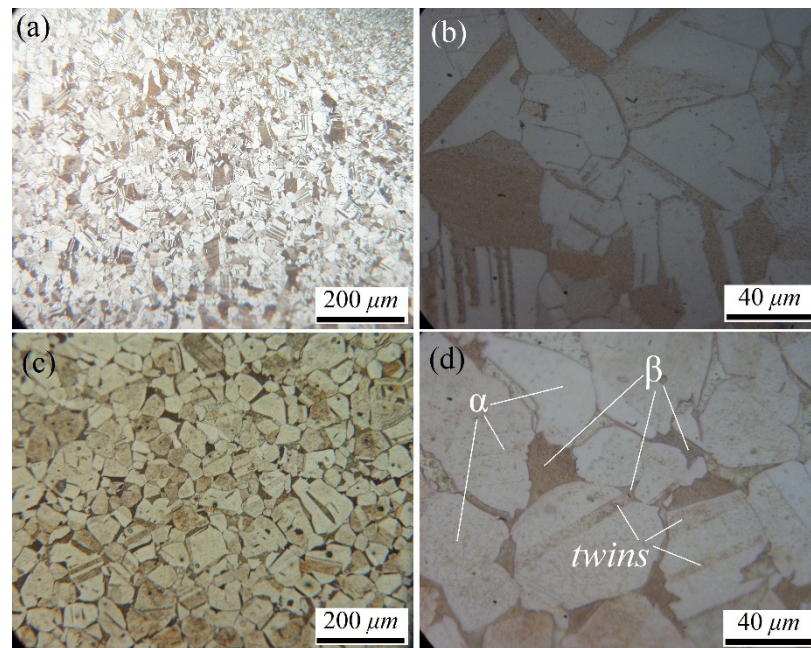


Figure 2. OM images of the single-phase (a,b) and double-phase (c,d) brasses at low and high magnifications. The magnification of (a,c) is $200\times$, and the magnification of (b,d) is $1000\times$.

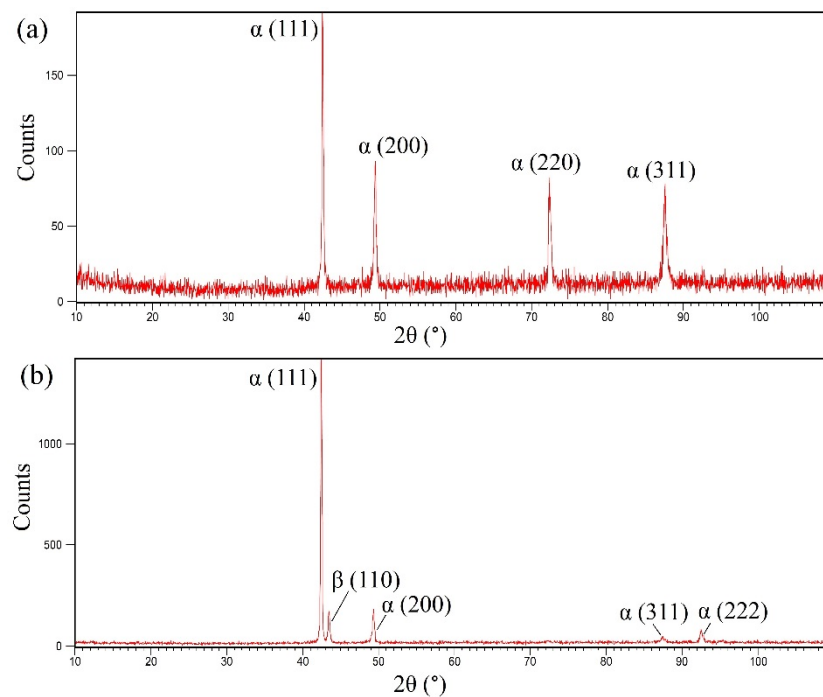


Figure 3. XRD results of the single-phase (a) and double-phase (b) brasses showing the β (110) peak after heat treatment in double-phase sample.

The inverse pole figure (IPF) map and phase map of the double-phase sample are shown in Figure 4, in which α and β phases are indicated by red and green colors, respectively. Figure 4 confirms the formation of larger β colonies at the primary α grain boundaries and finer β at the grain interiors. The higher magnification of the phase map of

the double-phase sample in conjunction with (110) and (111) pole figures of α and β at the interfacial areas (primary α grain boundary's zone) are depicted in Figure 5. Moreover, the highly magnified phase map of grain interiors and related (110) and (111) pole figures of α and β at the interfacial areas are illustrated in Figure 6.

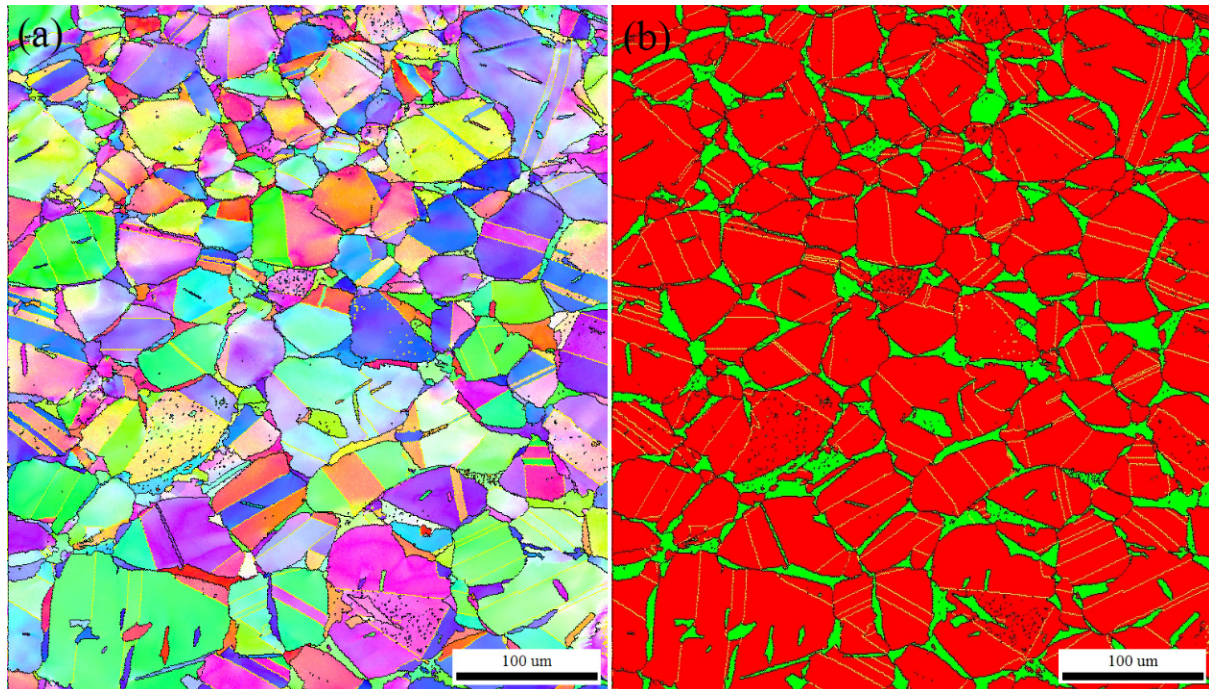


Figure 4. (a) IPF and (b) phase maps of the double-phase sample. The red and green colors in phase map refer to α and β phases, respectively.

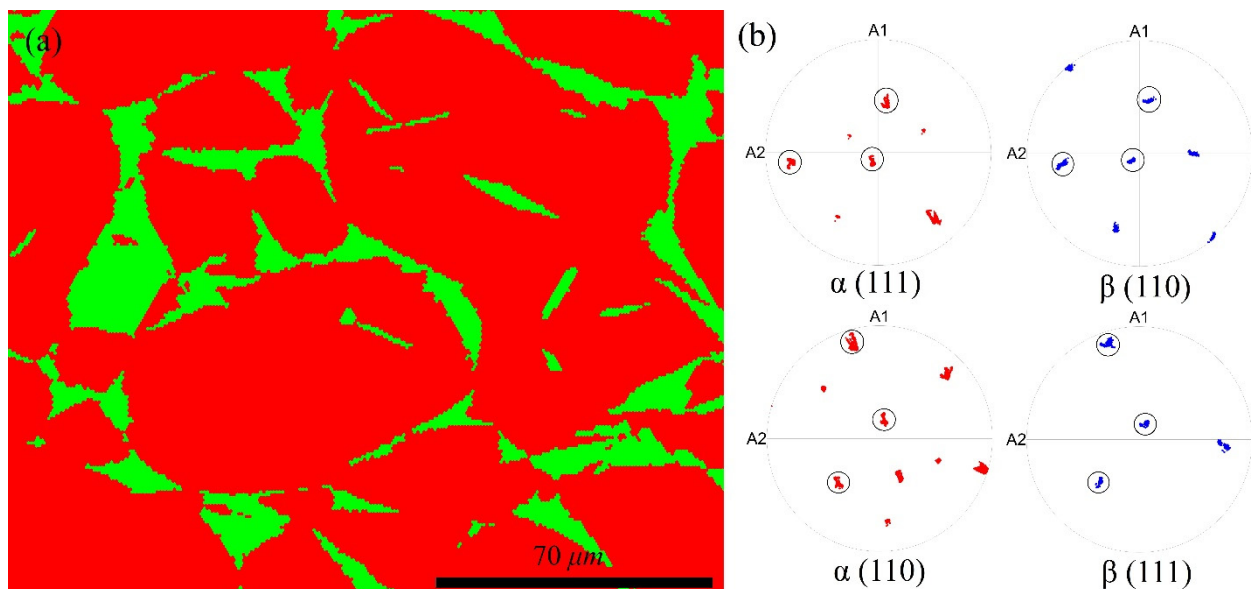


Figure 5. (a) Phase map of the double-phase sample at higher magnification. (b) (110) and (111) pole figures of α and β (formed at α primary grain boundaries) phases near the interfacial areas.

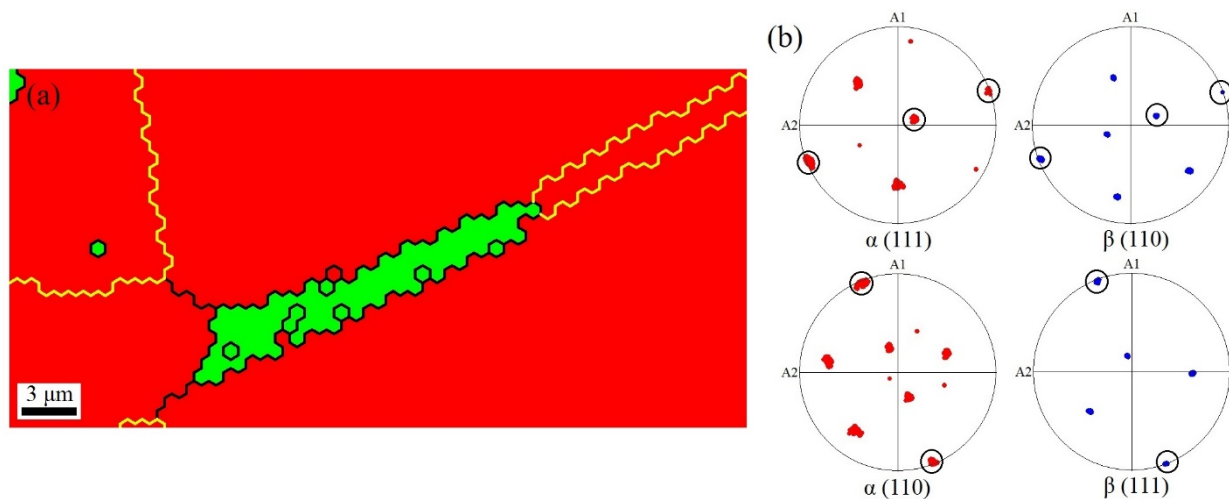


Figure 6. (a) Formation of β phase at $\Sigma 3$ twins boundaries at higher magnifications. (b) (110) and (111) pole figures of α and β (formed at $\Sigma 3$ twins boundaries) phases near the interfacial areas.

In Figures 5 and 6, pole figures designate the orientation relationship (OR) between α (FCC) and β (BCC) phases. From Figure 5, it can be seen that there is an OR in the regions of large β phases (at primary α grain boundaries) between $\{111\}_{FCC} // \{110\}_{BCC}$ and $\langle 110 \rangle_{FCC} // \langle 111 \rangle_{BCC}$. The OR during phase transformation of $FCC \leftrightarrow BCC$ structures have been investigated frequently, and it is well known that the possible ORs are as follows [5–7]:

- (1) $\{111\}_{FCC} // \{110\}_{BCC}, \langle 110 \rangle_{FCC} // \langle 111 \rangle_{BCC}$ (Kurdjumov–Sachs)
- (2) $\{001\}_{FCC} // \{001\}_{BCC}, \langle 110 \rangle_{FCC} // \langle 100 \rangle_{BCC}$ (Bain)
- (3) $\{111\}_{FCC} // \{110\}_{BCC}, \langle 211 \rangle_{FCC} // \langle 011 \rangle_{BCC}$ (Nishiyama–Wassermann)

According to Figure 5, the OR between α and disordered β at α primary grain boundaries was Kurdjumov–Sachs (KS) type.

In the case of grain interior (Figure 6), the $\Sigma 3$ twin boundaries (indicated by the yellow color in Figure 6a) are the preferred zones for $\alpha \rightarrow \beta$ phase transformation. As shown in Figure 6a, a $\Sigma 3$ twin boundary was partially transferred to a high-angle boundary (indicated by the black color) due to the formation of disordered β (BCC) within the twinned zone. On the other hand, the pole figures extracted from α and β phases adjacent to the $\Sigma 3$ twin boundary (Figure 6b) indicate the existence of a KS OR similar to α primary grain boundary zones. Therefore, the type of OR does not depend on the nucleation sites of the disordered β phase, and the $\alpha \rightarrow \beta$ phase transformation occurs under the KS relationship. Similar results have been reported by other researchers during phase transformation in brasses under different processing routes [8,9]. Zhao et al. [8] investigated the type of OR during $\alpha \rightarrow \beta$ phase transformation induced by electric current pulses in a brass alloy containing Cu 63.8 wt. % and Zn 36.2 wt. %. They concluded that the KS relationship is the most possible OR during $\alpha \rightarrow \beta$ phase transformation in brasses. Stanford and Bate [9] studied the type of OR during $\beta \rightarrow \alpha$ phase transformation during heat treatment. In their study, Widmanstätten α phase was grown from the primary β grain boundaries. Their results showed that the OR was close to the Young–Kurdjumov–Sachs relationship for α formation in β phase. The comparison between the results of this study with the literature [8,9] indicates two main points. First, the OR during $\alpha \rightarrow \beta$ phase transformation in brasses does not depend on the processing route. Second, the OR during $\alpha \rightarrow \beta$ and $\beta \rightarrow \alpha$ phase transformation in brasses does not alter, and in both cases, the Kurdjumov–Sachs relationship governs the microstructural evolution.

4. Conclusions

The phase-transformation-induced orientation relationship between the α and disordered β phase during heat treatment of a Cu-37 wt. % Zn alloy was investigated using electron backscattered diffraction. By heating a Cu-37 wt. % Zn single-phase alloy at 800 °C

for one hour, the primary α grains grew, and the β phase formed at suitable nucleation sites. The preferred nucleation sites for $\alpha \rightarrow \beta$ transformation are grain boundaries and grain interiors of the primary α phase. However, the more preferred zones are the grain boundaries in which the larger β phases are produced. It is worth noting that, at grain interior sites, the $\Sigma 3$ twins are the preferred sites for the nucleation of β phase. In the case of twin sites, the formation of a β phase destroys the $\Sigma 3$ special orientation and changes them to random, high-angle grain boundaries. The main orientation relationship induced by $\alpha \rightarrow \beta$ transformation is the Kurdjumov–Sachs relationship. Moreover, the Kurdjumov–Sachs relationship is not dependent on the type of β nucleation sites and processing routes.

Author Contributions: A.H.: methodology, investigation, formal analysis, writing—original draft; M.J.: conceptualization, methodology, formal analysis, writing—review and editing; L.S.-G.: conceptualization, methodology, validation, review and editing. All authors have read and agreed to the published version of the manuscript.

Funding: This research received no external funding.

Institutional Review Board Statement: Not applicable.

Informed Consent Statement: Not applicable.

Data Availability Statement: Not applicable.

Conflicts of Interest: The authors declare no conflict of interest.

References

1. Xu, N.; Song, Q.; Bao, Y. Investigation on microstructure development and mechanical properties of large-load and low-speed friction stir welded Cu-30Zn brass joint. *Mater. Sci. Eng. A* **2018**, *726*, 169–178. [[CrossRef](#)]
2. Heidarzadeh, A.; Mohammadzadeh, R. Developing α/β Laminar Composite Structure in CuZn Alloy by Heat Treatment and Submerged Friction Stir Processing. *Iran. J. Mater. Form.* **2021**, *8*, 26–32.
3. Rahimzadeh, A.; Heidarzadeh, A.; Mohammadzadeh, A.; Moeini, G. Effect of friction stir welding heat input on the microstructure and tensile properties of Cu-Zn alloy containing disordered β phase. *J. Mater. Res. Technol.* **2020**, *9*, 11154–11161. [[CrossRef](#)]
4. Heidarzadeh, A.; Chabok, A.; Klemm, V.; Pei, Y. A Novel Approach to Structure Modification of Brasses by Combination of Non-Equilibrium Heat Treatment and Friction Stir Processing. *Metall. Mater. Trans. A* **2019**, *50*, 2391–2398. [[CrossRef](#)]
5. Chapellier, P.; Ray, R.K.; Jonas, J.J. Prediction of transformation textures in steels. *Acta Metall. Mater.* **1990**, *38*, 1475–1490. [[CrossRef](#)]
6. Dames, G.J.; Kallend, J.S.; Morris, P.P. The quantitative prediction of transformation textures. *Acta Metall.* **1976**, *24*, 159–172. [[CrossRef](#)]
7. Tomida, T.; Wakita, M.; Yasuyama, M.; Sugaya, S.; Tomota, Y.; Vogel, S.C. Memory effects of transformation textures in steel and its prediction by the double Kurdjumov–Sachs relation. *Acta Mater.* **2013**, *61*, 2828–2839. [[CrossRef](#)]
8. Zhao, X.; Wang, X.L.; Li, D.X.; Dai, W.B. Orientation correlation during $\alpha \rightarrow \beta$ up-transformation induced by electric current pulses in a Cu-Zn alloy. *Mater. Sci. Forum Trans. Tech. Publ.* **2014**, *783–786*, 2406–2409. [[CrossRef](#)]
9. Stanford, N.; Bate, P.S. Crystallographic variant selection in $\alpha\text{-}\beta$ brass. *Acta Mater.* **2005**, *53*, 859–867. [[CrossRef](#)]